Rational Design of an Organocatalyst for Peptide Bond Formation

Handoko, Sakilam Satishkumar, Nihar R. Panigrahi and Paramjit S. Arora*

Department of Chemistry New York University, New York, NY 10003, U.S.A

ABSTRACT: Amide bonds are ubiquitous in peptides, proteins, pharmaceuticals and polymers. The formation of amide bonds is a relatively straightforward process: amide bonds can be synthesized with relative ease because of the availability of efficient coupling agents. However, there is a substantive need for methods that do not require excess reagents. A catalyst that condenses amino acids could have an important impact by reducing the significant waste generated during peptide synthesis. We describe the rational design of a biomimetic catalyst that can efficiently couple amino acids featuring standard protecting groups. The catalyst design combines lessons learned from enzymes, peptide biosynthesis, and organocatalysts. Under optimized conditions, 5 mol% catalyst efficiently couples Fmoc amino acids without significant racemization. Significantly, we demonstrate that the catalyst is functional for the synthesis of oligopeptides on solid phase. This result is significant because it illustrates the potential of the catalyst to function on a substrate with a multitude of amide bonds, which may be expected to inhibit a hydrogen bonding catalyst.

INTRODUCTION

Atom efficient construction of amide bonds has become an important challenge for organic chemists with the growing popularity of peptides as biological reagents and therapeutics. Contemporary approaches for peptide synthesis involve solid phase methodology,[1] which is a straightforward yet highly wasteful process, with typical conditions utilizing three to five equivalents of the coupling agents for every amide bond synthesized. Various potential approaches for catalyst driven peptide synthesis may be envisioned. Direct catalytic activation of carboxylic acids with amines would provide the most straightforward and efficient strategy. Catalytic activation of carboxylic acids with boronic acids and derivatives[2-6] and zirconium salts[7,8] has offered significant promise. Carboxylic acid esters, which are more electrophilic than carboxylic acids, provide an easily accessible alternative. Condensation of esters with amines catalyzed by Zr(OtBu)4,[9] ruthenium-PNN complex,[10] and N-heterocyclic carbenes[11] represent promising methods for obtaining amide bonds; however, here the esters must be pre-formed limiting the attractiveness of the approach. A recent report by Yamamoto and coworkers describes intriguing results with substrate-directed Lewis acid catalysts derived from titanium and tantalum.[12] Exciting approaches to obtain a native peptide bond from non-standard reaction partners and reaction pathways offer intriguing alternatives to carboxylic acids and esters. For example, the Staudinger ligation utilizes an amino acid phosphine and azido amino acid derivative to afford a native amide bond.[13,14] Tangible success has also been obtained with nonclassical approaches which include activation of reducible aldehydes with nucleophilic carbenes,[15,16] umpolung amide synthesis that employs oxidative coupling of bromonitroalkanes with amines,[17-19] and α-ketoacid—hydroxylamine condensation.[20,21]
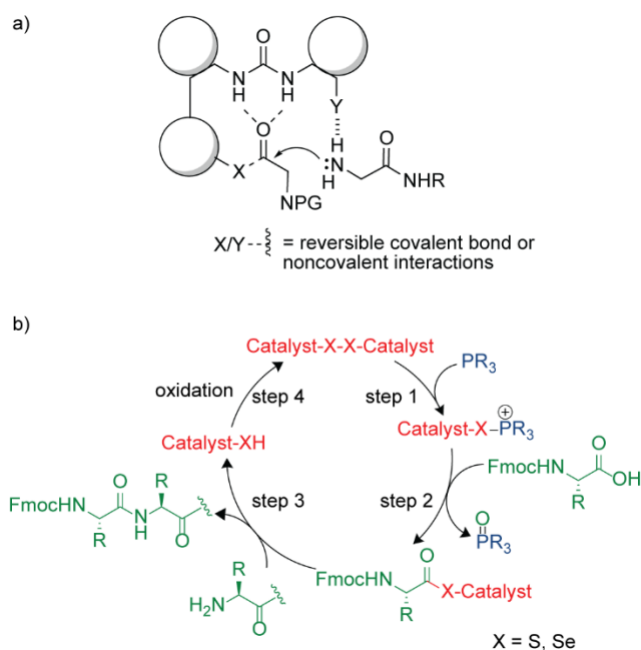

Figure 1. Idealized depiction of a catalyst that covalently or non-covalently engages the carboxylic acid and amine nucleophile to coax amide bond formation. PG = protecting group. b) Proposed

catalytic cycle for the activation and condensation of amino acids. The catalyst builds on a reduction-oxidation condensation protocol where a transient thioester or selenoester is formed between the catalyst and the amino acid.

The above discussion highlights the various approaches that are being pursued to develop an efficient catalyst for oligopeptide synthesis.[12,21-25] We sought to build an organocatalyst that would act upon Fmoc-amino acids—the standard monomers in peptide synthesis—with the hypothesis that for any new method to have significant impact on the practice of peptide synthesis, minimal changes to the existing protocols should be made. Our design builds on three biomimetic and synthetic precedents: (1) the

tetrahedral intermediate for amide bond formation that is stabilized by oxyanion holes in enzymes can be mimicked by urea catalysts. (2) Carboxylic acids are routinely activated as thioesters for synthesis of peptide bonds in nonribosomal peptide synthesis, and (3) thioesters can be readily accessed from carboxylic acids with disulfides and phosphorus (III) reagents, as described by Mukaiyama in 1970.[26] As illustrated in Figure 1, we sought to combine these important precedents with the concept of covalent catalysis. We envisioned a urea catalyst covalently linking to the carboxylic acid via a thioester bond; the thioester is then activated by the catalyst towards amide bond formation.
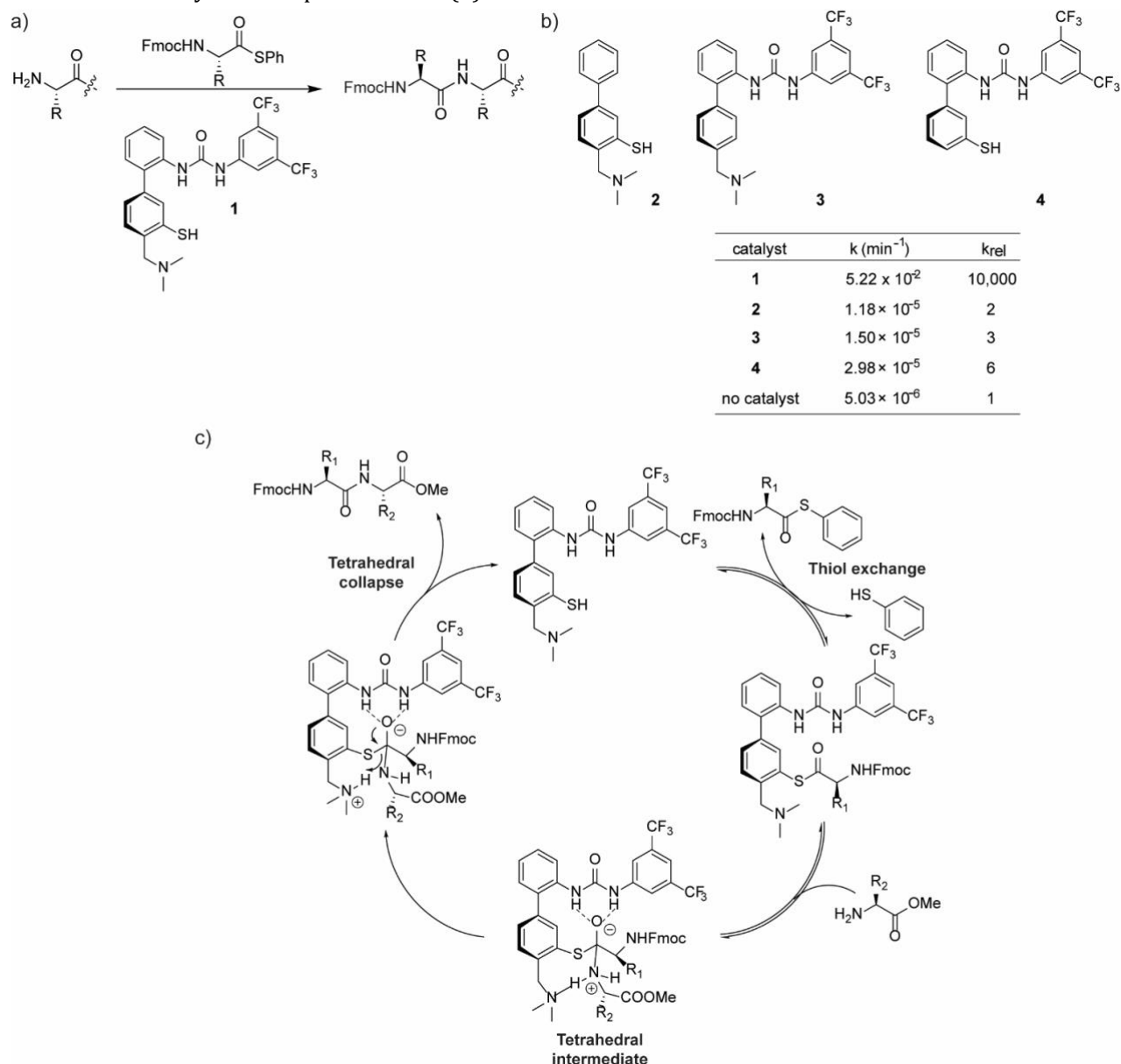

catalyst	k (min^{-1})	krel
1	5.22×10^2	10,000
2	1.18×10^{-5}	2
3	1.50×10^{-5}	3
4	2.98×10^{-5}	6
no catalyst	5.03×10^{-6}	1

Figure 2. (a) Urea **1** efficiently condenses amino acid thioesters with amines. (b) Pseudo first order rate constants for dipeptide formation with urea **1** and designed controls **2-4**.[27] The kinetics of the amidation reaction between Fmoc-

valine thiophenyl ester (10 mM) and alanine methyl ester (100 mM) in toluene are shown in the Table. The catalyst concentration was varied from 2.5 mol% to 10 mol%. (c) Proposed mechanism for amide bond formation catalyzed by catalyst **1**. The mechanism is supported by the previously reported studies.[27]

Our proposed catalytic cycle has four key steps (Figure 1b). The first and second steps involve the formation of an amino acid thioester from carboxylic acid, disulfide-linked catalyst dimer and a phosphorus (III) reagent. In the third step, the catalyst engages the amine nucleophile and the thioester to yield an amide bond. The catalyst-thiol, liberated from the prior step, then re-oxidizes to yield the disulfide for the next cycle. We developed several designs that originate from the proposed catalytic cycle. Here we illustrate the preliminary success of this concept for the efficient coupling of Fmoc-amino acids.

RESULTS

DESIGN OF AN ORGANOCATALYST THAT CONDENSES THIOESTERS WITH AMINES[27]

We began our studies by developing a catalyst from first principles that could accelerate condensation of thioesters with amines, i.e. Step 3 of the catalytic cycle in Figure 1b. We recently reported the iterative design of such a catalyst, which combines elements of protease active sites and lessons learned from peptide and protein ligation methodologies.[27] The salient results from the earlier study are shown in Figure 2. Briefly, the catalyst was designed to mimic the oxyanion hole to stabilize the tetrahedral intermediate.[28,29] Many hydrogen bonding scaffolds including ureas,[30] thioureas,[29,31] and squaramides[32,33] have been described for their potential to recognize anions. Several examples of hydrogen bonding catalysts aiding acylation or deacylation chemistries are also known.[34-41] We tested various scaffolds to arrive at the optimal urea catalyst **1**. The placement of the thiol and amine groups proved to be critical. Modeling studies suggested that the biphenyl/phenyl urea architecture provides the most favorable positioning for the thiol group in relation to the urea for efficient thioester exchange.[27] Tertiary alkyl amines proved to be superior bases. Figure 2b illustrates the dependence of the reaction on the urea group, the tertiary amine and thiol with negative controls **2-4** that are missing individual components. The controls show a significantly diminished rate for dipeptide bond formation between Fmoc-valine thiophenylester and alanine methyl ester supporting the hypothesis that a trifunctional catalyst is necessary for rate acceleration.

We envisioned two key steps in the catalytic amide bond formation by **1**: The first step involves a transthioesterification reaction between the thioester and **1**. This step is postulated to be mediated by hydrogen bonding with the urea group. The

catalyst•thioester complex then condenses with the amine leading to amide bond formation. We tested the dependence of the reaction on the concentration of the catalyst, thioester, and the amine moieties. Analysis suggests that amide bond formation is slower than transthioesterification. Careful ^{19}F NMR studies implicate the tertiary amine in both the transthioesterification and the amide bond formation steps. The postulated catalytic cycle supported by these extensive analyses is depicted in Figure 2c.

DEVELOPMENT OF A CATALYST THAT COUPLES CARBOXYLIC ACIDS AND AMINES

Catalyst **1** leads to an efficient formation of amide bonds from amino acid thioesters and amines. The above studies provide a foundation for our overall goal of developing a catalyst that directly couples amino acids. Our approach is based on the seminal work by Mukaiyama[26,42] and others[43,44] who have utilized a reduction–oxidation condensation procedure to synthesize amide bonds in a stoichiometric fashion.[44-47] We sought to make this approach more efficient by including a urea derivative as an oxyanion hole mimic to catalyze acyl transfer reactions.[28,29,34-39]

Our goal requires the catalyst to first self-condense with the carboxylic acid to form a thioester followed by amide bond formation (Figure 1). Thioesters can be accessed from carboxylic acids with disulfides and phosphorus (III) reagents.[26] We utilized tributylphosphine in these initial studies after a preliminary investigation with different phosphines. The oxidized form of the catalyst provides the requisite disulfide.

We tested the potential of the disulfide form of **1**, denoted as **1-S** in Figure 3, to couple toluic acid and benzylamine, as model carboxylic acid and amine substrates for the formation of Amide **A**. Detailed conditions for the model reaction are: toluic acid (10 μmol), benzylamine (20 μmol), catalyst (0.5 μmol, 5 mol%), tributylphosphine (15 μmol), and 3Å molecular sieves (30% w/v) in 1 mL acetonitrile at room temperature. The reaction progress was monitored by HPLC and percent conversion to amide **A** in comparison to an internal standard is reported. We used millimolar concentrations of the carboxylic acid and amine because these concentrations are common in peptide synthesis.
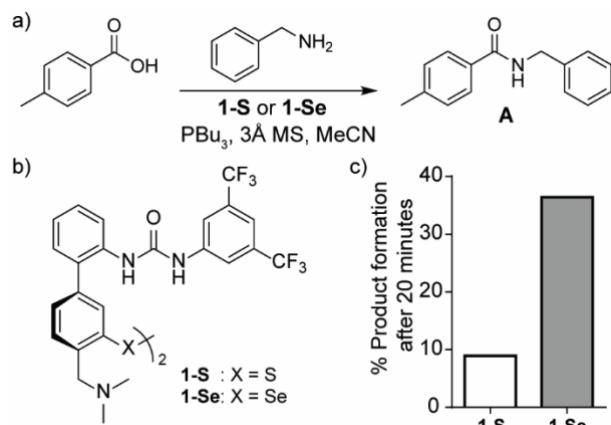
Figure 3. Formation of Amide **A** after 20 minutes under unoptimized reaction conditions: toluic acid (10 µmol), benzylamine (20 µmol), catalyst (0.5 µmol, 5 mol%), tributylphosphine (15 µmol), and 3Å molecular sieves (50% w/v) in 1 mL acetonitrile. Reactions were conducted at room temperature under open air.
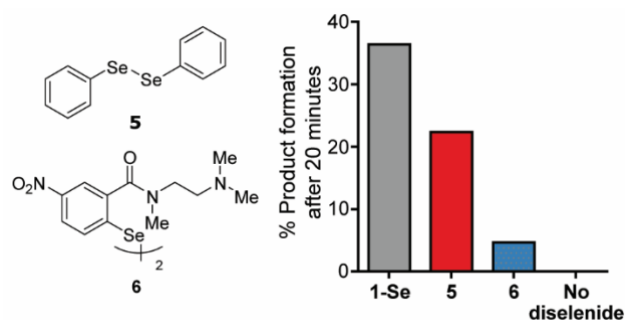

Figure 4. Comparison of **1-Se** to diselenide controls **5** and **6** under the same reaction conditions as in Figure 3 with 5 mol% of each diselenide. No reaction is observed in the absence of a diselenide.

Gratifyingly, we found that 5 mol% **1-S** provides 9% amide formation after 20 minutes and the product formation slowly increases to 65% after 4 hours (Supporting Information, Figure S1). We next sought to improve upon this initial success by testing the performance of the diselenide derivative **1-Se**. We postulated that the selenium substitution may lead to a more efficient catalyst due to the rate enhancement provided by the diselenide in the selenoester and amide formation[48] steps as well as in the reoxidation step to regenerate the diselenide (Step 3 in Figure 1).[49] Diselenide **1-Se** leads to 36% product formation after 20 minutes, which is a significant overall rate enhancement over **1-S**.

We synthesized and evaluated two control diselenides to gauge the contribution of the different components– the urea, tertiary amine and the diselenide – that comprise catalyst **1-Se**. We compared the rates of the amide bond formation with diphenyldiselenide **5** and diselenide **6**. The latter derivative was recently described[50] by Liebeskind and coworkers as part of their own significant efforts to develop an acylative oxidation–reduction condensation system for amide bond formation.[43,50,51] Both **5** and **6** serve as diselenide controls for **1-Se**, with **6** also featuring a tertiary amine base. Both derivatives allow us to gauge the contribution from the designed urea component. Figure 4 demonstrates the effectiveness of **1-Se** as compared to the diselenide analogs. Under the same reaction condition as described above, diphenyldiselenide leads to roughly 20% product formation after 20 minutes while diselenide **6** is less effective. As expected, no reaction is seen in the absence of a diselenide.

Design of Macrocyclic Catalysts to Enhance Reoxidation

The above results provide a foundation for further optimization of our designs. Although **1-Se** leads to higher product formation than diphenyldiselenide, the difference is not significant. Importantly, we observed that while most of the diselenides tested offer a burst in product formation over 20-30 minutes, reaction progress stalls after this initial rate enhancement (Supporting Information, Figure S1). Many side reactions that lead to the decomposition of the starting materials and phosphine reagent can be envisioned; however, we postulated that oxidation of the selenol to the diselenide (Step 3 of the catalytic cycle in Figure 1b) might be slow thus limiting catalyst availability for the subsequent steps. We envisioned that the rate of the diselenide formation could be enhanced by linking the individual selenol units to increase their effective concentration for oxidation. Accordingly, we synthesized several macrocyclized analogs of **1-Se** (Figure 5). We chose to access the macrocycle by linking the individual selenol units through the tertiary amine group because the amine base and the diselenide group are attached to the same aromatic ring.
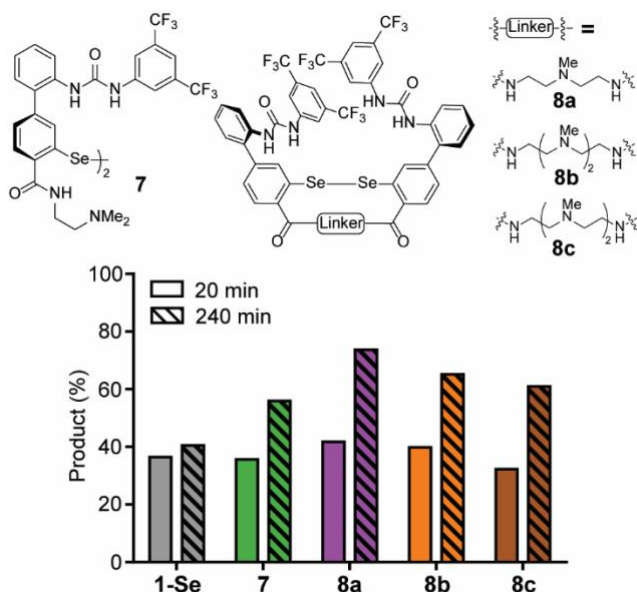
Figure 5. Comparison of diselenides 1-Se and 7 to macrocyclic diselenides 8a–8c for catalysis of A under the same reaction conditions as reported in Figure 3 caption. Bar graphs depict product formation after 20 and 240 minutes with 5 mol% catalyst.

We began by redesigning **1-Se** to simplify the synthesis: the alkyl tertiary amine base was appended to the biphenyl group through an amide bond so we could optimize the linker length by appending dialkylamines of different lengths. We synthesized diselenide **7** as a control for **1-Se** and compared its activity to the parent compound after 20 and 240 minutes. Roughly 40% of Amide **A** is formed in the presence of 5 mol% **1-Se** after 20 minutes, with little further increase observed after 240 minutes. With 5 mol% diselenide **7**, we observe an enhancement to 60% product formation after 240 minutes. Replacement of the alkyl amine appendage from **1-Se** to the electron-withdrawing amide group in **7** lowers the pKa of the ortho-selenol group, potentially accounting for the change in the reaction profile.

We next used three bis-amino linkers of varying lengths to prepare macrocyclic derivatives **8a-8c**. We designed **8a-8c** such that the tertiary amine will remain equidistant in all three scaffolds. Notably, these compounds exist as mixture of oligomers of dimer that once reduced, become chemically equivalent. (Supporting information, Figure S6–S7) The profiles of these macrocycles are compared to **1-Se** and **7** in Figure 5. Macrocyclization provided further boost leading to roughly 70% product formation after 4 h, with **8a** proving to be the most efficient catalyst.
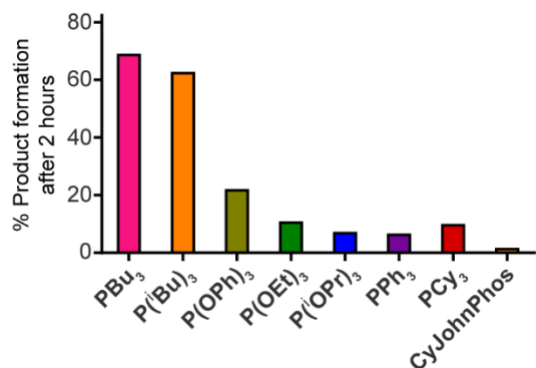

Figure 6. Evaluation of phosphine and phosphites as reaction partners for 8a. Less congested trialkylphosphines – PBu_3 and $P(iBu)_3$ – provided the highest yields of A after 2 hours under the same reaction conditions as listed in Figure 3 caption.

Optimization of the Reaction Conditions for Organocatalyst 8a

Encouraged by the above results, we next evaluated reaction conditions to optimize the performance of **8a**. We employed tributylphosphine during the initial catalyst screening. Repeated studies with different diselenides suggested that reaction progress stalled due to premature depletion of PBu_3 (Supporting Information, Figure S2). We hypothesized that PBu_3 is oxidized during the reaction, thus limiting catalytic efficiency. We anticipated that the use of less air-sensitive phosphines may lead to better reaction yield.

We screened various phosphines and phosphites with diverse steric and electronic properties to identify an optimal reaction partner for **8a** (Figure 6). Electron density at the phosphorus center of phosphines is related to their sensitivity towards air oxidation.[52] Disappointingly, we found that the more oxidatively stable PPh_3 leads to only 6% product after 2 hours as compared to 70% with PBu_3 under the same reaction conditions. We also screened electronically rich but sterically bulky phosphines such as PCy_3 and CyJohnPhos but found similarly low yield of product **A**.[53] $P(iBu)_3$, which has similar electronic properties to PBu_3 produced similar yield.

To identify a phosphorus(III) derivative that is less sensitive to oxidation yet has similar steric properties to that of PBu_3, we next shifted our attention to $P(OPh)_3$, which has a similar Tolman cone angle to that of PBu_3.[54] We found that reaction employing $P(OPh)_3$ was slow (20% product formation after 2 hours, Figure 6). Similar results were also observed with other phosphites such as $P(OEt)_3$ and $P(OiPr)_3$. This result indicates that the electronic properties of P(III) reagents play important roles in affecting the turnover rate of the reaction. An electron-rich and less bulky

P(III) reagent is likely necessary to achieve efficient catalyst turnover; however, these properties also cause the reagent to be air sensitive. Tributylphosphine straddles the middle ground between activity and resistance to oxidative degradation and proved to be a suitable reducing partner for catalyst **8a**.

We next optimized each reaction component and parameter, including solvent, temperature, time, the dehydrating agent, and concentrations of the starting carboxylic acid, amine, tributylphosphine, and catalyst **8a** (Table 1). The reaction progress was monitored by HPLC and percent conversion to amide **A** in comparison to an internal standard is reported. We sought to determine the highest conversion to the product under each reaction condition within 24 hours of monitoring. In many cases, the reaction progress halts before reaching full conversion, as discussed earlier; in these instances, the time required to reach the maximal conversion is noted. We found the reaction to be the highest yielding in polar aprotic solvents such as acetonitrile and DMF, with acetonitrile providing faster conversion (Table 1, Entries 1-6). We attribute this observation to DMF, which features a hydrogen-bond acceptor, competing with the urea moiety of **8a**. These solvents are typically used in peptide synthesis and suitable for dissolving protected amino acids.

A dehydrating agent is critical for the reaction progress, as is also the case for catalytic Mitsunobu reactions.[55-57] We surveyed various molecular sieves, alumina and anhydrous magnesium sulfate (Entries 7-13), and found that 4 Å molecular sieves lead to the highest conversion.

Phosphine oxidation is a limiting factor in the reaction progress. We determined the highest amount of tributylphosphine required for quantitative conversion of toluic acid to the product. At millimolar substrate concentrations, such as those employed in standard peptide synthesis protocols, three equivalents of tributylphosphine lead to near quantitative yield of the amide **A** in four hours (Entry 16). We tested the impact of slow addition of phosphine on reaction progress. As expected, addition of fresh batches of phosphine reduces its total amount required in the reaction. Addition of 0.5 equivalent of phosphine in three batches leads to enhanced conversion to **A** (Entries 17-19). Lastly, we found that an increase in reaction temperature to 60 °C provides further boost to near quantitative conversion. *Under optimized conditions, 2.5-5 mol% **8a** catalyzes efficient condensation of equimolar amounts of carboxylic acid and amine partners (Entries 20-22).*

Table 1. Optimization of reaction conditions with **8a**.

Entry	Toluic Acid (mM)	Benzylamine (mM)	Catalyst (% mol)	PBu$_3$ (mM)	Dehydrating Agent[a] (% w/v)	Temperature	Solvents[b]	%Conversion to **A**
1	10	20	5%	15	3Å MS (50%)	RT	MeCN	76% (6 h)
2							DMF	75% (24 h)
3							Dioxane	24% (6 h)
4							THF	22% (6 h)
5							Toluene	1% (24 h)
6							DCE	25% (6 h)
7	10	20	5%	15	4Å MS (50%)	RT	MeCN	75% (2 h)
8					5Å MS (50%)			59% (1 h)
9					13X MS (50%)			13% (24 h)
10					Alumina (50%)			No reaction
11					MgSO$_4$ (50%)			20% (6 h)
12					None			36% (10 min)
13					4Å MS (30%)			76% (1 h)
14	10	20	5%	20	4Å MS (30%)	RT	MeCN	85% (2 h)
15				25				95% (4 h)
16				30				99% (4 h)
17	10	20	5%	3 × 5[d]	4Å MS (30%)	RT	MeCN	90% (2 h)
18	10	10	5%	3 × 5[d]	4Å MS (30%)	RT	MeCN	90% (2 h)
19	20	10	5%	3 × 5[d]	4Å MS (30%)	RT	MeCN	76% (2 h)
20	**10**	**10**	**5%**	**3 × 5[d]**	**4Å MS (30%)**	**60°C**	**MeCN**	**99% (1.5 h)**
21			2.5%					97% (4 h)
22			1%					21% (6 h)

ANALYSIS OF THE MECHANISM OF AMIDE BOND CATALYSIS BY 8a

We rigorously analyzed the kinetics of the reaction with respect to four different components – catalyst **8a**, toluic acid, benzylamine, and tributylphosphine – to gain insight into the mechanism of the reaction. The reoxidation of selenols to diselenide is mediated by atmospheric oxygen; we regarded oxygen concentration as a constant in our calculations. The kinetic studies and the proposed catalytic mechanism are shown in Figure 7 and Supporting Information Figure S37–S46. We analyzed the impact of varying concentrations of each component on the initial rate of the reaction. We also utilized the variable time normalization analysis described by Burés to determine reaction orders for each component (Supporting Information).[58-60]

Reaction profiles at various catalyst concentrations (0.5–1.5 mM) were obtained. Plotting of product concentration against normalized time [**8a**]$_n$ t reveals a first-order dependence on catalyst **8a**. Diselenide **8a** is a dimer and urea-based organocatalysts often show a tendency to form higher order aggregates,[61-65] but

our analysis suggests that only one molecule of reduced **8a** (or any of its intermediates) is involved in the rate determining step of the reaction.

Similar analysis for toluic acid also revealed first-order dependence on the carboxylic acid component of the reaction at lower concentration (5–12 mM). At higher concentrations, saturation kinetics was observed as evidence from the plateauing of initial rate versus toluic acid concentration curve (Supporting Information, Figure S44). This behavior is consistent with rapid association and dissociation of the
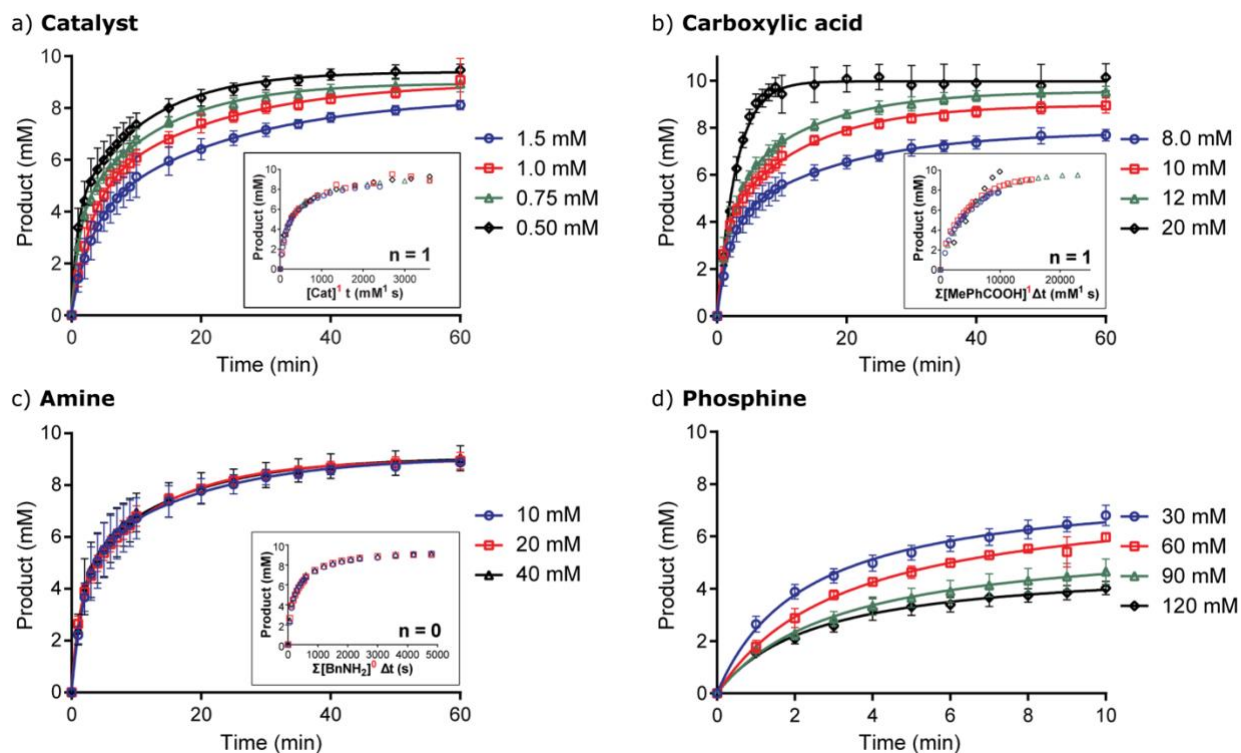

Figure 7. Dependence of reaction rate on concentrations of (a) catalyst **8a**, (b) toluic acid, (c) benzylamine, and (d) tributylphosphine. Variable time normalization analysis was utilized to elucidate the reaction orders from concentration profiles of the reaction (insets in panels a-c).
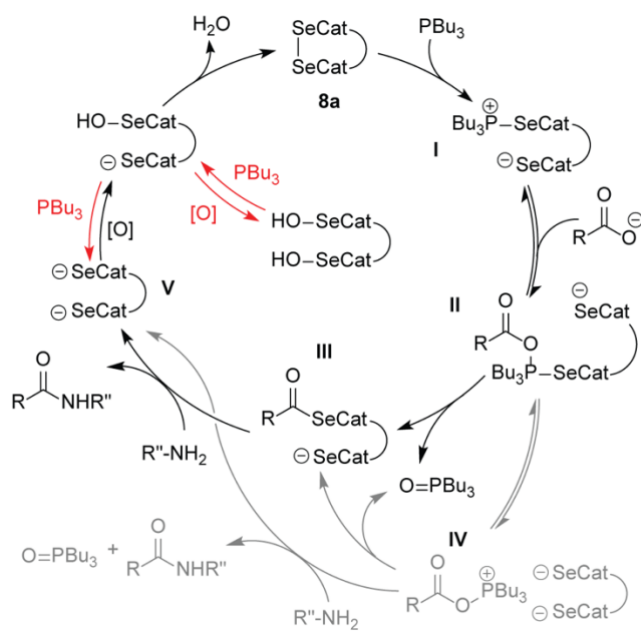

Figure 8. The proposed mechanism, supported by the kinetic studies, is shown in black. The possible side reactions are depicted in red and gray fonts.

carboxylate and selenophosphonium (Figure 7e: **I-II**). The saturation kinetics at higher carboxylate concentrations suggest that any of the succeeding reaction steps may be rate limiting.

We observed no rate dependence on amine concentration, implying that nucleophilic attack of amine to activated ester is fast and kinetically irrelevant. Owing to exceptional nucleophilicity of selenolates and in analogy to mechanism of PyBOP mediated coupling,[66,67] we hypothesize the involvement of selenoester intermediate (**III**) in the amide bond formation step. The observation that the reaction rate slows considerably when reaction solvent is changed from acetonitrile to DMF (Table 1, Entries 1 and 2 and Supporting Information, Figure S12) suggests that the assistance of hydrogen bonding from the urea moiety is necessary for fast conversion.

Formation of the selenoester intermediate has also been implicated by Singh, *et al.* in amide bond formation with stoichiometric tributylphosphine and diphenyldiselenide.[46]

Analysis of the initial rates of reaction with varying tributylphosphine concentration (30–120 mM) suggests that the reaction has a negative one-half rate order dependence on phosphine (Supporting Information, Figure S46). We rationalize this peculiar result to denote the complex role of tributylphosphine in the reaction, which includes its sensitivity to oxidation. Beyond the desired role of the phosphine for catalyst reduction, we hypothesize that it also inhibits catalyst reoxidation, presumably by reacting with selenenic acid to form tributylphosphine oxide and bis-selenolate V.

Table 2. Potential of diselenide 8a to catalyze coupling diverse Fmoc-protected amino acids into dipeptides.
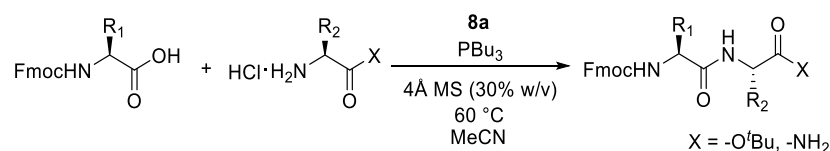
Entry	Dipeptides	Catalyst (% mol)	Method A: Slow Addition of Phosphine[b] (% Conversion[d])	Method B: One Pot Reaction[c] (%Conversion[d])	Epimerization[e]
1	FmocAlaAlaOtBu	2.5%	86% (1 h)[f]	-	dr > 99:1
2		5.0%	97% (1 h)[f, h]	92% (1 h)	
3	FmocAlaPheOtBu	5.0%	95% (1 h)[f]	99% (30 min)	
4	FmocAlaLys(Z)OtBu	5.0%	99% (1.5 h)[g]	98% (1 h)	
5	FmocAlaValOtBu	5.0%	99% (1 h)[f]	96% (1 h)	
6	FmocAlaProOtBu	5.0%	94% (2 h)[g]	69% (1 h)	
7	FmocAlaTrpNH$_2$	5.0%	99% (1 h)[f]	73% (1 h)	
8	FmocPheAlaOtBu	5.0%	90% (1 h)[f]	87% (30 min)	
9	FmocLys(Boc)AlaOtBu	5.0%	90% (1 h)[f]	90% (30 min)	
10	FmocProAlaOtBu	5.0%	90% (2 h)[g]	82% (30 min)	
11	FmocArg(Pbf)AlaOtBu	5.0%	99% (1.5 h)[g]	89% (1 h)	
12	FmocValAlaOtBu	5.0%	92% (2 h)[g]	81% (30 min)	dr = 99 :1
13	FmocAibAlaOtBu	5.0%	91% (2 h)[g]	53% (1.5 h)	
14	FmocPheProOtBu	5.0%	82% (2 h)[g]	-	dr = 98 :2

[a]Reaction condition: Fmoc-Xaa-OH (10 μmol), HCl•H-Xaa-OtBu or HCl•H-Xaa-NH$_2$ (11 μmol), DIEA (11 μmol), **8a**, PBu$_3$, 4Å MS (300 mg), in 1 mL ACN at 60°C. [b]Method A: Two or three portions of PBu$_3$ (5 μmol per portion) were added every 30 minutes. [c]Method B: PBu$_3$ (11 μmol) was added in one portion. [d]Conversions were monitored by HPLC using biphenyl as internal standard. Time to reach maximum conversion is provided in parentheses. [e]The amount of epimerization was quantified by HPLC. [f]Reaction reached maximum conversion after two 5-μmol portions of PBu$_3$ were added. [g]Reaction required three 5-μmol portions of PBu$_3$ to reach maximum conversion. [h]The isolated yield for a 0.2 mmol scale synthesis of Fmoc-AlaAlaOtBu is 90%.

Based on our analysis and literature precedence,[46,68-71] we propose the catalytic cycle outlined in Figure 8. The diselenide catalyst **8a** is reduced by tributylphosphine to form selenophosphonium **I**, which associates rapidly with the carboxylate to form the pentacoordinated phosphorane **II**. Intramolecular acyl transfer of **II** leads to selenoester **III** and concomitant release of tributylphosphine oxide. Rapid aminolysis of **III** leads to formation of the desired amide product and release

of bis-selenolate **V**, which oxidizes back to catalyst **8a** on exposure with air. Water and hydrogen peroxide molecules produced as side products from selenolate oxidation are absorbed and decomposed respectively by molecular sieves.55,57 Alternative mechanisms that involve direct nucleophilic attack by the amine on acyloxyphosphonium intermediate (**IV**) or exchange of the acyloxyphosphonium back to selenoesters may also be in play. The kinetic analysis suggests that the catalyst reoxidation is the slow step in the cycle.

CATALYST 8a EFFICIENTLY COUPLES AMINO ACIDS

Our overall goal is to develop catalysts that act on protected amino acids routinely used in solid phase synthesis. We rationalized that a sub-stoichiometric reagent that can couple Fmoc amino acids protected with standard protecting groups would be useful in reducing waste in peptide synthesis. Toward this end, we tested the potential of **8a** on substrates beyond the model compounds described above (Table 2).

We began by analyzing the rate of alanine dipeptide formation. Commercially available amino acid esters or amides were directly used. These amino acids are available as HCl salts and equimolar *N,N*-diisopropylethylamine was added to the reaction mixture to scavenge the acid. Condensation of 10 mM Fmoc-alanine with 11 mM alanine *t*-butyl ester in acetonitrile leads to 86% yield of Fmoc-Ala-Ala-O-*t*-Bu dipeptide with 2.5 mol% **8a** after 1 hour (Table 2, Entry 1). The yield of the dipeptide product increases to 97% with 5 mol% 8a (Table 2, Entry 2). These examples utilized slow addition of tributylphosphine in two 5-μmol portions (Method A in Table 2). One pot addition of 1.1 equivalent of tributylphosphine with 5 mol% **8a** provided 92% conversion (Method B) – a slight decrease from the slow addition method but still a highly encouraging result. We tested various amino acid partners for Fmoc-alanine to gauge the scope of the catalyst. We surveyed aromatic amino acids (phenylalanine and tryptophan), protected lysine, valine and proline (Table 2, Entries 3-7). In each case, high yields for the dipeptide products were obtained. We were particularly gratified to learn that the catalyst can couple amino acids with β-branching and secondary amine.

We next explored different Fmoc-amino acids as the coupling partners (Table 2, Entries 8-13). We tested phenylalanine, lysine and arginine with standard side chain protecting groups, valine, proline and aminoisobutyric acid (Aib). Fmoc-Aib provides a stringent test for probing the role of amino acid sterics on catalytic efficiency. We were pleased to learn that catalyst **8a** can lead to a high conversion to the dipeptide in every case; although, the bulkier amino acids valine and Aib required longer reaction times.

Epimerization of amino acids is a major concern in peptide synthesis. To rigorously quantify the amount of potential epimerization resulting from the catalyst-mediated product formation step, we prepared both LL and DL epimer of FmocAlaAlaO*t*Bu and FmocValAlaO*t*Bu dipeptides. We also tested coupling of Fmoc-phenylalanine and proline-t-Bu, two non-alanine amino acids that react slowly, to assess the impact of the slow reaction on epimerization (Table 2, Entry 14). Careful analysis showed less than 2% epimerization under the reaction conditions for any of the dipeptides tested (Table 2, Figure 9 and Supporting Information, Figure S3–S5).

Catalyst Mediated Solid Phase Peptide Synthesis

We next evaluated the potential of **8a** to catalyze solid phase peptide synthesis. We were interested in testing the potential of the catalyst on solid phase because a catalyst that functions through hydrogen bonding interactions and coordination with carbonyl groups would be expected to be less efficient with peptide substrates as compared to amino acids due to the presence of multiple carbonyl groups and other coordinating sites. As a proof of concept, we aimed to synthesize a pentapeptide (Fmoc-FEKAG-NH2) on resin using standard
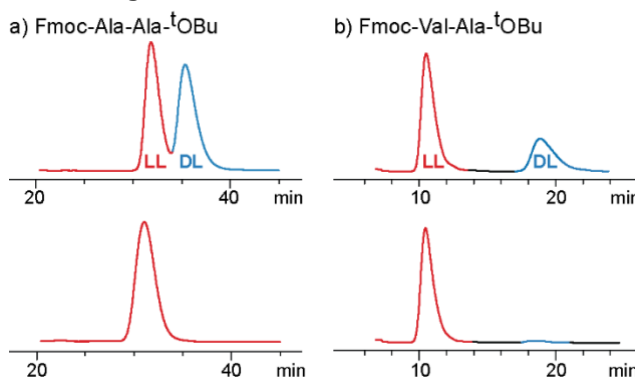

Figure 9. HPLC studies to determine potential epimerization during peptide coupling mediated by **8a**. (a) Comparison of HPLC traces of authentic sample of racemic FmocAlaAlaO*t*Bu (top) and that of crude reaction mixture (bottom). (b) Comparison of HPLC traces of authentic sample of (LL)-FmocValAlaO*t*Bu spiked with (DL)-FmocValAlaO*t*Bu (top) and that of crude reaction mixture (bottom). HPLC condition: Chiralcel®OD 250 × 4.6 mm column; isocratic elution of 5% isopropanol in hexanes; flow rate = 1.0 mL/min; detection wavelength = 280 nm.
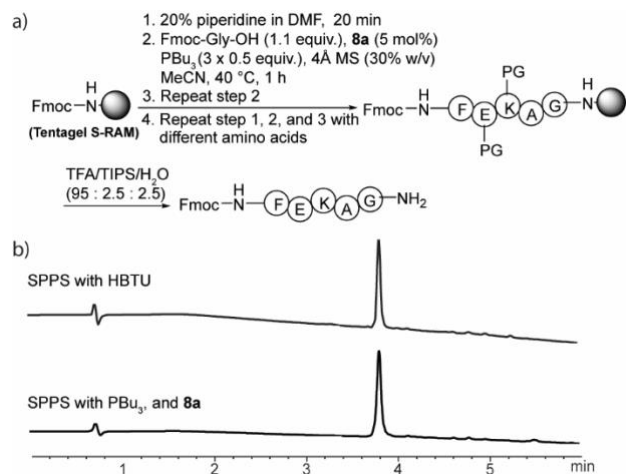
Figure 10. (a) Protocol for solid phase synthesis mediated by PBu3 and 8a. (b) HPLC traces of crude peptide FmocFEKAG-NH2 synthesized using HBTU (top) and PBu3 and **8a**(bottom). HPLC condition: Poroshell 120 EC-C18 4.6 × 100 mm 2.7 μm column; 0.1% TFA (v/v) in water (solvent A): acetonitrile (solvent B); gradient 5–100% (solvent B) in 6 min; flow rate = 1.5 mL/min; detection wavelength = 220 nm.

Fmoc-amino acids. The reaction progress was monitored using the Kaiser test which indicates incomplete coupling of resin-bound free amines. We utilized 1.1 equivalent of the Fmoc-amino acid and 5 mol% of **8a** in this study. After each coupling step, molecular sieves were separated from the resin support by use of buoyant force. As the peptide becomes longer (beyond 3 residues), the complete reaction of the free amine required two coupling cycles. The pentapeptide prepared using **8a** and standard coupling agents were then cleaved from resin and analyzed by HPLC. Spectra of the crude cleaved products indicate that relatively pure peptide was obtained after iterative synthesis on solid phase. The same peptide synthesized using standard coupling agent HBTU is provided as control (Figure 10b). Despite the inconveniences, the performance of the catalyst for solid phase peptide synthesis (SPPS) is highly encouraging.

CONCLUSION

We describe efforts to develop an organocatalyst for amide bond formation from commercially available Fmoc amino acids featuring standard side chain protecting groups. The catalyst design builds on urea-based hydrogen bonding scaffolds and the concept of covalent catalysis. The proposed catalytic cycle utilizes a reduction–oxidation condensation procedure to activate the carboxylic acid as a selenoester. The diselenide required for this transformation is a component of the catalyst. The selenoester linkage reversibly connects the amino

acid to the organocatalyst which catalyzes amide bond formation.

The studies described here provide a lead towards *catalytic peptide synthesis*. We utilized an iterative design approach to develop a macrocyclic diselenide catalyst that yields near quantitative conversion of carboxylic acids and amines to their amide products under optimized conditions. The catalyst is active on a diverse range of amino acid substrates and shows promise for solid phase peptide synthesis. Insignificant epimerization of chiral amino acids was observed in the catalyzed reaction. The result with oligomer synthesis is particularly rewarding because hydrogen bonding catalysts may not be expected to be efficient in the presence of multiple amide bonds.

The overall aim of this work is to develop organocatalysts that can replace standard coupling agents in commercial synthesizers, and limit waste in peptide synthesis. This goal will require further optimization. Specifically, we need to limit the dependence on a drying agent and explore phosphorus (III) reagents that are less prone to oxidation. We are continuing to evaluate other phosphine derivatives, to overcome the limitations imposed by tributylphosphine. Our initial investigations utilized a catalytic cycle that requires oxidation of stoichiometric amounts of a phosphine. In continuing studies, we are exploring recycling of the phosphine oxide product so as to achieve a catalytic cycle that includes catalytic amounts of phosphines. Silanes have recently been used as reagent for reducing phosphine oxides to phosphines in catalytic Mitsunobu reactions.56 The results of these ongoing investigations will be reported in due course.

ASSOCIATED CONTENT

The Supporting Information is available free of charge on the ACS Publications website.
Synthesis, characterization, kinetic studies, and spectroscopy data (PDF)

AUTHOR INFORMATION

Corresponding Author

*arora@nyu.edu

REFERENCES

(1) Merrifield, R. B. *J. Am. Chem. Soc.* **1963**, *85*, 2149.
(2) Charville, H.; Jackson, D.; Hodges, G.; Whiting, A. *Chem. Commun.* **2010**, *46*, 1813.
(3) Ishihara, K.; Ohara, S.; Yamamoto, H. *J. Org. Chem.* **1996**, *61*, 4196.

(4) Georgiou, I.; Ilyashenko, G.; Whiting, A. *Acc. Chem. Res.* **2009**, *42*, 756.

(5) Al-Zoubi, R. M.; Marion, O.; Hall, D. G. *Angew. Chem. Int. Ed.* **2008**, *47*, 2876.

(6) Noda, H.; Furutachi, M.; Asada, Y.; Shibasaki, M.; Kumagai, N. *Nat Chem* **2017**, *9*, 571.

(7) Allen, C. L.; Chhatwal, A. R.; Williams, J. M. J. *Chem. Commun.* **2012**, *48*, 666.

(8) Lundberg, H.; Tinnis, F.; Adolfsson, H. *Chem. Eur. J.* **2012**, *18*, 3822.

(9) Han, C.; Lee, J. P.; Lobkovsky, E.; Porco, J. A. *J. Am. Chem. Soc.* **2005**, *127*, 10039.

(10) Gnanaprakasam, B.; Milstein, D. *J. Am. Chem. Soc.* **2011**, *133*, 1682.

(11) Movassaghi, M.; Schmidt, M. A. *Org. Lett.* **2005**, *7*, 2453.

(12) Muramatsu, W.; Hattori, T.; Yamamoto, H. *J. Am. Chem. Soc.* **2019**, *141*, 12288.

(13) Nilsson, B. L.; Kiessling, L. L.; Raines, R. T. *Org. Lett.* **2000**, *2*, 1939.

(14) Saxon, E.; Armstrong, J. I.; Bertozzi, C. R. *Org. Lett.* **2000**, *2*, 2141.

(15) Vora, H. U.; Rovis, T. *J. Am. Chem. Soc.* **2007**, *129*, 13796.

(16) Bode, J. W.; Sohn, S. S. *J. Am. Chem. Soc.* **2007**, *129*, 13798.

(17) Shen, B.; Makley, D. M.; Johnston, J. N. *Nature* **2010**, *465*, 1027.

(18) Schwieter, K. E.; Johnston, J. N. *ACS Catalysis* **2015**, *5*, 6559.

(19) Schwieter, K. E.; Shen, B.; Shackleford, J. P.; Leighty, M. W.; Johnston, J. N. *Org. Lett.* **2014**, *16*, 4714.

(20) Bode, J. W.; Fox, R. M.; Baucom, K. D. *Angew Chem Int Ed Engl* **2006**, *45*, 1248.

(21) Pattabiraman, V. R.; Bode, J. W. *Nature* **2011**, *480*, 471.

(22) de Figueiredo, R. M.; Suppo, J.-S.; Campagne, J.-M. *Chem. Rev.* **2016**, *116*, 12029.

(23) Krause, T.; Baader, S.; Erb, B.; Gooßen, L. J. *Nature Communications* **2016**, *7*, 11732.

(24) Sabatini, M. T.; Boulton, L. T.; Sheppard, T. D. *Science Advances* **2017**, *3*, e1701028.

(25) Liu, Z.; Noda, H.; Shibasaki, M.; Kumagai, N. *Org. Lett.* **2018**, *20*, 612.

(26) Endo, T.; Ikenaga, S.; Mukaiyama, T. *Bull. Chem. Soc. Jpn.* **1970**, *43*, 2632.

(27) Wu, H.; Handoko; Raj, M.; Arora, P. S. *Org. Lett.* **2017**, *19*, 5122.

(28) Doyle, A. G.; Jacobsen, E. N. *Chem. Rev.* **2007**, *107*, 5713.

(29) Zhang, Z.; Schreiner, P. R. *Chem. Soc. Rev.* **2009**, *38*, 1187.

(30) Curran, D. P.; Kuo, L. H. *J. Org. Chem.* **1994**, *59*, 3259.

(31) Blain, M.; Yau, H.; Jean-Gérard, L.; Auvergne, R.; Benazet, D.; Schreiner, P. R.; Caillol, S.; Andrioletti, B. *ChemSusChem* **2016**, *9*, 2269.

(32) Alemán, J.; Parra, A.; Jiang, H.; Jørgensen, K. A. *Chem. Eur. J.* **2011**, *17*, 6890.

(33) Malerich, J. P.; Hagihara, K.; Rawal, V. H. *J. Am. Chem. Soc.* **2008**, *130*, 14416.

(34) Jarvo, E. R.; Copeland, G. T.; Papaioannou, N.; Bonitatebus, P. J.; Miller, S. J. *J. Am. Chem. Soc.* **1999**, *121*, 11638.

(35) Pratt, R. C.; Lohmeijer, B. G. G.; Long, D. A.; Waymouth, R. M.; Hedrick, J. L. *J. Am. Chem. Soc.* **2006**, *128*, 4556.

(36) Ema, T.; Tanida, D.; Matsukawa, T.; Sakai, T. *Chem. Commun.* **2008**, 957.

(37) Müller, C. E.; Schreiner, P. R. *Angew. Chem. Int. Ed.* **2011**, *50*, 6012.

(38) Kheirabadi, M.; Çelebi-Ölçüm, N.; Parker, M. F. L.; Zhao, Q.; Kiss, G.; Houk, K. N.; Schafmeister, C. E. *J. Am. Chem. Soc.* **2012**, *134*, 18345.

(39) Matsumoto, M.; Lee, S. J.; Waters, M. L.; Gagné, M. R. *J. Am. Chem. Soc.* **2014**, *136*, 15817.

(40) Jaegle, M.; Steinmetzer, T.; Rademann, J. *Angew. Chem. Int. Ed.* **2017**, *56*, 3718.

(41) Mandai, H.; Fujii, K.; Yasuhara, H.; Abe, K.; Mitsudo, K.; Korenaga, T.; Suga, S. *Nature Communications* **2016**, *7*, 11297.

(42) Mukaiyama, T. *Angew Chem Int Ed Engl.* **1976**, *15*, 94.

(43) Liebeskind, L. S.; Gangireddy, P.; Lindale, M. G. *J. Am. Chem. Soc.* **2016**, *138*, 6715.

(44) Ghosh, S. K.; Singh, U.; Mamdapur, V. R. *Tetrahedron Lett.* **1992**, *33*, 805.

(45) Mukaiyama, T.; Matsueda, R.; Maruyama, H.; Ueki, M. *J. Am. Chem. Soc.* **1969**, *91*, 1554.

(46) Singh, U.; Ghosh, S. K.; Chadha, M. S.; Mamdapur, V. R. *Tetrahedron Lett.* **1991**, *32*, 255.

(47) Liu, R.; Orgel, L. E. *Nature* **1997**, *389*, 52.

(48) Raj, M.; Wu, H.; Blosser, S. L.; Vittoria, M. A.; Arora, P. S. *J. Am. Chem. Soc.* **2015**, *137*, 6932.

(49) Reich, H. J.; Hondal, R. J. *ACS Chem. Biol.* **2016**, *11*, 821.

(50) Akondi, S. M.; Gangireddy, P.; Pickel, T. C.; Liebeskind, L. S. *Org. Lett.* **2018**, *20*, 538.

(51) Gangireddy, P.; Patro, V.; Lam, L.; Morimoto, M.; Liebeskind, L. S. *J. Org. Chem.* **2017**, *82*, 3513.

(52) Barder, T. E.; Buchwald, S. L. *J. Am. Chem. Soc.* **2007**, *129*, 5096.

(53) Wolfe, J. P.; Singer, R. A.; Yang, B. H.; Buchwald, S. L. *J. Am. Chem. Soc.* **1999**, *121*, 9550.

(54) Tolman, C. A. *Chem. Rev.* **1977**, *77*, 313.

(55) Hirose, D.; Taniguchi, T.; Ishibashi, H. *Angew. Chem. Int. Ed.* **2013**, *52*, 4613.

(56) Buonomo, J. A.; Aldrich, C. C. *Angew. Chem. Int. Ed.* **2015**, *54*, 13041.

(57) März, M.; Chudoba, J.; Kohout, M.; Cibulka, R. *Org. Biomol. Chem.* **2017**, *15*, 1970.

(58) Burés, J. *Angew. Chem. Int. Ed.* **2016**, *55*, 16084.

(59) Burés, J. *Angew. Chem. Int. Ed.* **2016**, *55*, 2028.

(60) Nielsen, C. D. T.; Burés, J. *Chemical Science* **2019**, *10*, 348.

(61) Zafar, A.; J. Geib, S.; Hamuro, Y.; D. Hamilton, A. *New Journal of Chemistry* **1998**, *22*, 137.

(62) Oh, S. H.; Rho, H. S.; Lee, J. W.; Lee, J. E.; Youk, S. H.; Chin, J.; Song, C. E. *Angew. Chem. Int. Ed.* **2008**, *47*, 7872.

(63) Obrzud, M.; Rospenk, M.; Koll, A. *Physical Chemistry Chemical Physics* **2014**, *16*, 3209.

(64) Ford, D. D.; Lehnherr, D.; Kennedy, C. R.; Jacobsen, E. N. *J. Am. Chem. Soc.* **2016**, *138*, 7860.

(65) Salvio, R.; Massaro, L.; Puglisi, A.; Angelini, L.; Antenucci, A.; Placidi, S.; Sciubba, F.; Galantini, L.; Bella, M. *Org. Biomol. Chem.* **2018**, *16*, 7041.

(66) Coste, J.; Frerot, E.; Jouin, P. *J. Org. Chem.* **1994**, *59*, 2437.

(67) Hudson, D. *J. Org. Chem.* **1988**, *53*, 617.

(68) Lattanzi, A. In *Comprehensive Organic Synthesis II (Second Edition)*; Elsevier: Amsterdam, 2014, p 837.

(69) Iwaoka, M.; Tomoda, S. In *Organoselenium Chemistry: Modern Developments in Organic Synthesis*; Wirth, T., Ed.; Springer Berlin Heidelberg: Berlin, Heidelberg, 2000, p 55.

(70) Kei, G.; Keiichi, S.; Michiko, N.; Renji, O.; Takayuki, K. *Chemistry Letters* **2003**, *32*, 1080.

(71) Schwartz Radatz, C.; Rampon, D. S.; Balaguez, R. A.; Alves, D.; Schneider, P. H. *Eur. J. Org. Chem.* **2014**, *2014*, 6945.

Table of Contents artwork